Geol. Mag. **151** (*3*), *2014*, *pp. 430–446*. © *Cambridge University Press 2013*
doi:10.1017/S0016756813000307

The status of the Makrotantalon Unit (Andros, Greece) within the structural framework of the Attic-Cycladic Crystalline Belt

MAGDALENA H. HUYSKENS*‡† & MICHAEL BRÖCKER*

*Institut für Mineralogie, Westfälische Wilhelms-Universität Münster, Corrensstr. 24, 48149 Münster, Germany
‡Present address: Research School of Earth Sciences, The Australian National University, Bldg 142 Mills Road, 0200 Canberra, ACT, Australia

(*Received* 10 September 2012; *accepted* 20 March 2013; *first published online* 19 July 2013)

Abstract – This study focuses on the status of the Makrotantalon Unit (Andros, Greece) within the framework of the Cycladic nappe stack. We document unambiguous evidence that this unit has experienced blueschist-facies metamorphism and identify previously unknown lawsonite ± pumpellyite assemblages in glaucophane-free metasediments. The position of the presumed tectonic contact at the base of this unit is vague, but roughly outlined by serpentinites. Only a single outcrop displays a weak angular unconformity with cohesive cataclasites in the footwall. Rb–Sr geochronology was carried out on 11 samples representing various rock types collected within or close to inferred or visible fault zones. Owing to a lack of initial isotopic equilibration and/or subsequent disturbance of the Rb–Sr isotope systematics, isochron relationships are poorly developed or non-existing. In NW Andros, direct dating of distinct displacement events has not been possible, but a lower age limit of ~ 40 Ma for final thrusting is constrained by the new data. Sporadically preserved Cretaceous ages either indicate regional differences in the *P–T–d* history or a different duration of metamorphic overprinting, which failed to completely eliminate inherited ages. The detachment on the NE coast records a later stage of the structural evolution and accommodates extension-related deformation. Apparent ages of ~ 29–25 Ma for samples from this location are interpreted to constrain the time of a significant deformation increment. On a regional scale, the Makrotantalon Unit can be correlated with the South Evia Blueschist Belt, but assignment to a specific subunit is as yet unconfirmed.

Keywords: Makrotantalon Unit, Andros, Cyclades, Attic-Cycladic Crystalline Belt, Greece, Rb–Sr geochronology.

1. Introduction

The Attic-Cycladic Crystalline Belt (ACCB) in the central Aegean region (Fig. 1) represents a major tectonostratigraphic unit of the Hellenides. The complex geological, magmatic and tectonometamorphic evolution of this area documents the closure of a Neotethyan ocean basin and associated subduction- and collision-related processes in Cenozoic time that result from convergence between the Apulian microplate and the Eurasian continent. Subsequently, an extensional tectonic setting developed in the context of the southward retreat of the Hellenic subduction zone and the westward-directed extrusion of the Anatolian plate that had been induced by the Arabia–Eurasia collision (e.g. Gautier *et al*. 1999; Ring *et al*. 2010). Two major groups of tectonic units can be distinguished, which represent a diverse suite of distinct crustal segments with contrasting geological and metamorphic histories. For simplicity, these groups are referred to as the Upper Cycladic Unit, which has not been affected by high-pressure/low-temperature (HP/LT) metamorphism, and the Cycladic Blueschist Unit, respectively, each consisting of different fault-bounded units that are separated by low-angle normal faults (e.g. Dürr *et al*. 1978; Okrusch & Bröcker, 1990; Gautier & Brun, 1994*a, b*; Avigad *et al*. 1997). Owing to preservation of many key features, the ACCB allows the study of practically all aspects of orogenesis and has therefore attracted much attention from the geoscience community. The general geological, tectonic and metamorphic framework has been documented in numerous studies. However, owing to the fragmentary outcrop pattern as well as complex litho- and/or tectonostratigraphic relationships, regional correlations across the Cycladic archipelago are often only broadly constrained (e.g. Keay & Lister, 2002; Bröcker & Pidgeon, 2007; Gärtner *et al*. 2011). Unravelling of the structural framework is further complicated by the fact that for some parts of the larger study area only large-scale maps and/or results of reconnaissance investigations are available. Several important issues are still poorly constrained, e.g. the internal architecture of the tectonic stacks that build up the two main groups, regional similarities and correlations between individual tectonic units, the nature of major shear zones that separate individual units and the age of lateral displacement along these tectonic contacts. Clarification of these aspects is a necessary prerequisite for in-depth understanding of the geodynamic history and refinement of related models.

This study focuses on the island of Andros (Fig. 1). Its central geographical position and good rock

†Author for correspondence: magda.huyskens@anu.edu.au

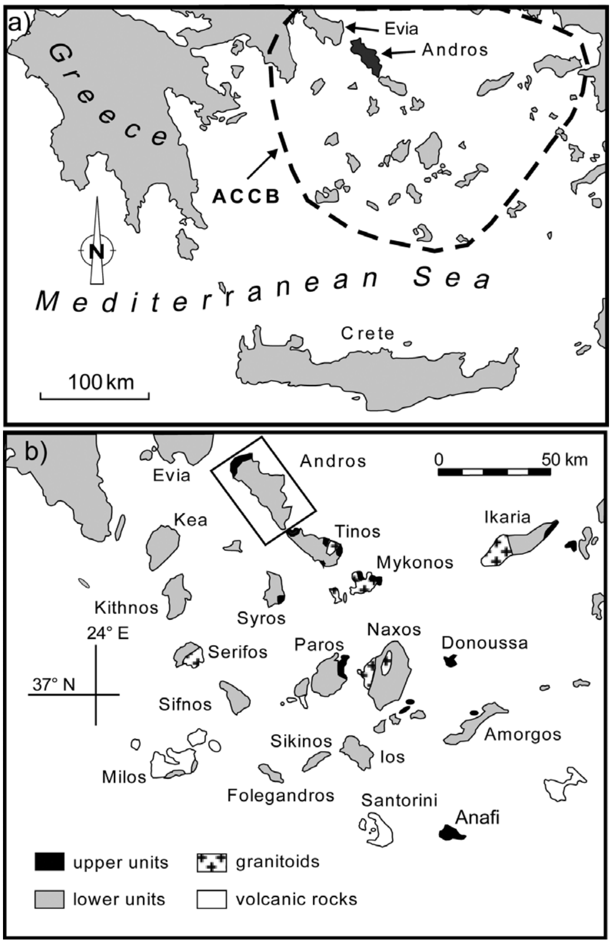

Figure 1. (a) Regional overview and (b) simplified geological map of the Cycladic archipelago (modified after Matthews & Schliestedt, 1984).

exposure offer the excellent opportunity to address its lithological and structural relationships with the neighbouring islands (Evia and Tinos), possibly providing new insights into the crustal architecture of the Cyclades. Two tectonic units, the Makrotantalon Unit and the Lower Unit of Central-Southern Andros, were identified in previous studies (e.g. Papanikolaou, 1978*b*). Within the structural framework of the ACCB, the Lower Unit can unambiguously be correlated with the Cycladic blueschist sequences. In contrast, the status of the Makrotantalon Unit is unclear and its geological significance and tectonometamorphic affinity is controversial (Papanikolaou, 1978*b*, 1987; Dürr, 1986; Bröcker & Franz, 2006; Mehl *et al.* 2007). Various interpretations include the assumption that the Makrotantalon Unit belongs either to the Cycladic HP/LT sequences (e.g. Papanikolaou, 1978*b*, 1987) or to the Upper Unit (Dürr, 1986; Bröcker & Franz, 2006), or represents an intermediate unit juxtaposed between both (Mehl *et al.* 2007). This paper addresses this controversy and attempts to unravel the structural position and importance of the Makrotantalon Unit though a combination of field observations, petrographic and mineralogical studies and Rb–Sr dating of rocks collected close to the inferred tectonic contact. Special emphasis has been placed on the questions: Did blueschist-facies metamorphism affect the Makrotantalon Unit? Is it possible to identify unambiguous field evidence for tectonic juxtaposition of the Makrotantalon Unit onto the Cycladic blueschist sequences and if so, is it possible to date shear zone activity? Furthermore, we were interested in possible deformation-related effects on the Rb–Sr system caused by tectonic displacement along a detachment located in the topmost part of the Lower Unit that is considered to be unrelated to the Makrotantalon Unit – Lower Unit juxtaposition (Mehl *et al.* 2007).

2. Geological background

2.a. Regional setting

Detailed overviews of the main geological and petrological features of the ACCB have been reported by Dürr *et al.* (1978), Dürr (1986), Okrusch & Bröcker (1990) and Ring *et al.* (2010). Therefore, only a short summary of the characteristics most relevant for the present study is given here.

The Upper Cycladic Unit is only preserved in small areas (Fig. 1b) and comprises unmetamorphosed Permian to Mesozoic sediments, ophiolites, greenschist- to amphibolite-facies rocks and Late Cretaceous granitoids (e.g. Dürr *et al.* 1978; Patzak, Okrusch & Kreuzer, 1994; Zeffren *et al.* 2005), which have been emplaced by low-angle detachments onto the Cycladic Blueschist Unit (e.g. Avigad & Garfunkel, 1989). The Upper Cycladic Unit lacks evidence for a HP stage, which is a key feature in the metamorphic evolution of the structurally lower sequences. Most metamorphic rocks yielded Cretaceous ages (e.g. Patzak, Okrusch & Kreuzer, 1994), but some studies have shown that at least parts of the hangingwall sequence record the imprint of a Miocene greenschist-facies event (Bröcker & Franz, 1998; Zeffren *et al.* 2005).

The Cycladic Blueschist Unit is built up by a pre-Alpidic basement, which is overlain by a metamorphosed continental margin sequence of Permo-Mesozoic age (e.g. Dürr *et al.* 1978; Okrusch & Bröcker, 1990), mainly comprised of clastic metasediments, calcschists, marbles and metabasic rocks. This cover also includes mélanges with meta-igneous blocks and tectonic slabs (< 1 m to several hundred metres) that are enclosed in an ultramafic or metasedimentary matrix (e.g. Katzir *et al.* 2000; Bröcker & Keasling, 2006). The Cycladic Blueschist Unit experienced at least two stages of Tertiary metamorphism. During the first stage, eclogite- to epidote-blueschist-facies conditions were reached ($T = \sim 450$–$550\,°C$, $P = \sim 12$–20 kbar; e.g. Bröcker *et al.* 1993; Trotet, Vidal & Jolivet, 2001). In the northern and central Cyclades, subsequent overprinting occurred at greenschist-facies conditions ($T = \sim 450$–$550\,°C$, $P = \sim 4$–9 kbar; e.g. Bröcker *et al.* 1993; Parra, Vidal & Jolivet, 2002), whereas the southern Cyclades (e.g. Naxos) experienced amphibolite-facies metamorphism and partial melting (e.g. Buick & Holland, 1989). Regional

https://doi.org/10.1017/S0016756813000307 Published online by Cambridge University Press

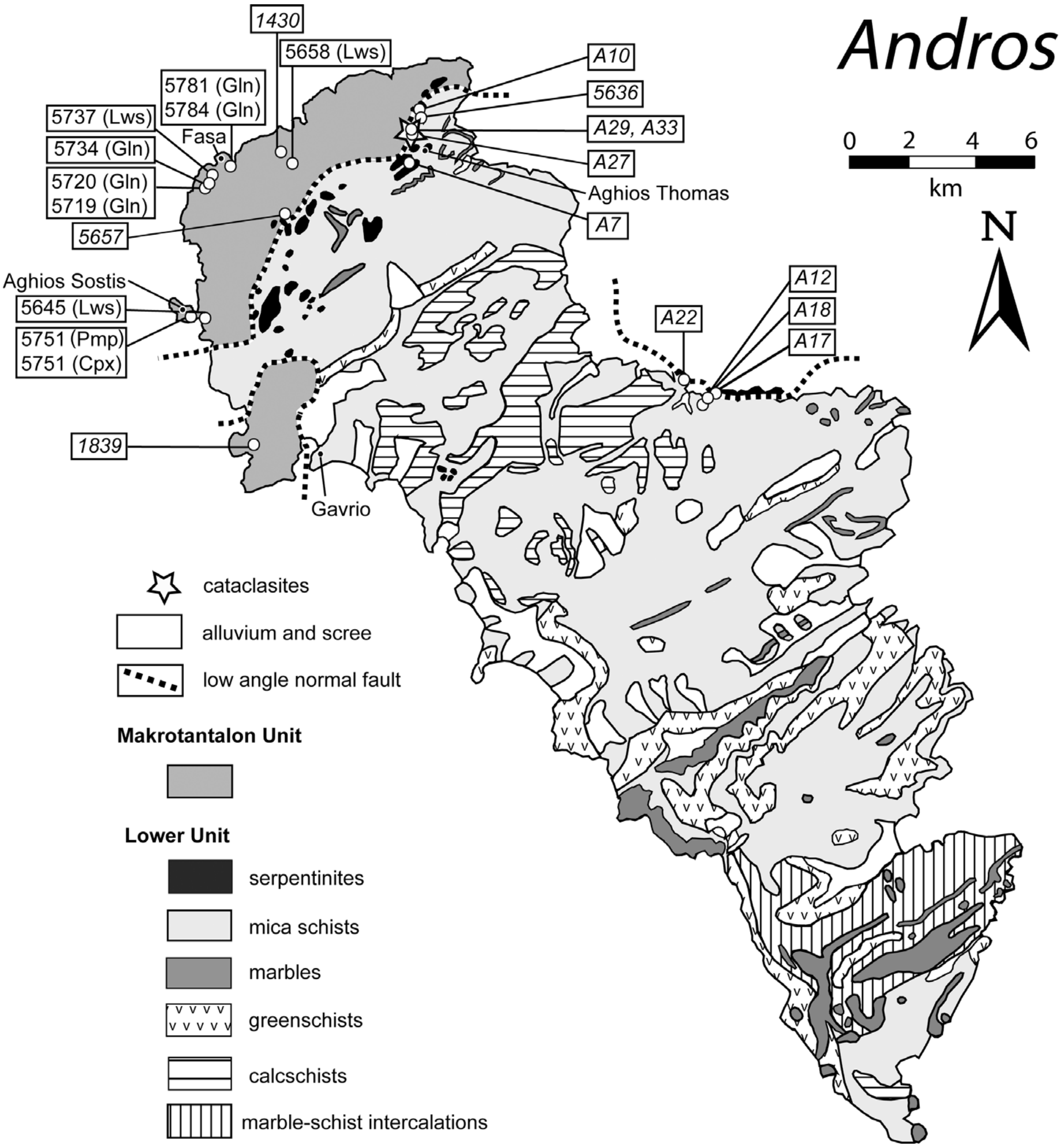

Figure 2. Simplified geological map of Andros (modified after Papanikolaou, 1978*a*; Bröcker & Franz, 2006 and Mehl *et al*. 2007) with key petrographic and geochronologic sample locations. (Cpx – clinopyroxene; Gln – glaucophane; Lws – lawsonite; Pmp – pumpellyite.)

metamorphism was followed by widespread intrusion of granitoids (e.g. Altherr *et al*. 1982). HP/LT rocks mostly yielded Eocene (55–40 Ma) metamorphic ages, whereas those of greenschist- to amphibolite-facies rocks ranged from late Oligocene to Miocene in age (~ 25–16 Ma; e.g. Altherr *et al*. 1979, 1982; Wijbrans & McDougall, 1988; Wijbrans, Schliestedt & York, 1990; Bröcker *et al*. 1993, 2004; Bröcker & Franz, 1998, 2005, 2006; Putlitz, Cosca & Schumacher, 2005). The importance of Cretaceous HP/LT metamorphism (~ 80 Ma; Bröcker & Enders, 1999; Bröcker & Keasling, 2006) has not yet been unambiguously documented (Bulle *et al*. 2010; Fu *et al*. 2010).

2.b. Local geology

On Andros (Fig. 2), the metamorphic succession can be subdivided into at least two tectonic units, the Lower Unit of Central-Southern Andros and the Makrotantalon Unit (Papanikolaou, 1978*b*). The Lower Unit (up to 1200 m thick) is correlative with the Cycladic blueschist sequences and mainly consists of clastic metasediments, carbonate-rich schists, marbles and metavolcanic rocks (Papanikolaou, 1978*b*). Ion probe U–Pb zircon dating of intercalated felsic metavolcanic rocks indicated Triassic protolith ages (~ 240–249 Ma; Bröcker & Pidgeon, 2007). Mineral assemblages document severe greenschist-facies metamorphism, but relict HP rocks are sporadically preserved (Reinecke, Okrusch & Richter, 1985; Dekkers *et al*. unpub. data; Buzaglo-Yoresh, Matthews & Garfunkel, 1995). Disrupted bodies of ultramafic, metagabbroic and meta-acidic rocks (up to several hundred metres in length) were recognized at various lithostratigraphic levels, representing meta-olistostromes, tectonic mélanges and/or macroboudins (e.g.

https://doi.org/10.1017/S0016756813000307 Published online by Cambridge University Press

Papanikolaou, 1978*b*; Mukhin, 1996; Bröcker & Pidgeon, 2007). Ion probe U–Pb zircon dating of a meta-gabbro and a gneiss yielded Jurassic protolith ages (~ 154–160 Ma; Bröcker & Pidgeon, 2007). Available *P–T* data for the Lower Unit suggests a minimum pressure of > 10 kbar at temperatures of ~ 450–500 °C (Reinecke, 1986; Buzaglo-Yoresh, Matthews & Garfunkel, 1995). *P–T* conditions for the greenschist-facies overprint were estimated at 350–520 °C and 5–9 kbar (Reinecke, 1982; Bröcker & Franz, 2006). Rb–Sr phengite dating yielded the same range in ages as determined elsewhere in the Cycladic Blueschist Unit for HP rocks (~ 50–40 Ma) and their retrograde derivatives (~ 23–21 Ma) (Bröcker & Franz, 2006). According to Mehl *et al.* (2007), the island belongs to the group of metamorphic core complexes exposed in the Aegean area. NE-trending folds formed within the stability field of glaucophane, after the peak HP metamorphism and simultaneously with the early stage of retrogression in the context of a constrictional strain regime during regional NE–SW extension (Ziv *et al.* 2010).

The structurally higher Makrotantalon Unit (up to 600 m thick) mainly consists of clastic metasediments and marbles. Metabasic schists are of subordinate importance. Fossils in dolomitic marbles yielded Permian ages (Papanikolaou, 1978*b*). The Makrotantalon Unit is mainly exposed in the northern part of the island. Greenschist-facies mineral assemblages are widespread but the *P–T* evolution is poorly constrained. Available data suggests temperatures of 350–455 °C at 4.1–5.4 kbar (Bröcker & Franz, 2006). An earlier HP stage (Reinecke, 1982) is uncertain, because unambiguous indications for blueschist- to eclogite-facies metamorphism were not recognized in subsequent studies (Papanikolaou, 1978*b*; Bröcker & Franz, 2006). Rb–Sr white mica geochronology indicated apparent ages between ~ 104 and ~ 21 Ma and led to the conclusion that the Makrotantalon Unit had experienced two distinct episodes of metamorphism in Cretaceous (~ 100–90 Ma and ~ 80–70 Ma) and Miocene (~ 24–21 Ma) times (Bröcker & Franz, 2006).

The exact position of the inferred tectonic contact at the base of the Makrotantalon Unit is difficult to localize, but is roughly marked by serpentinites. These were interpreted by Papanikolaou (1978*b*) to represent a distinct horizon within the Lower Unit based on lithostratigraphic observations. Biostratigraphic evidence suggests that the rocks of the Makrotantalon Unit are older than those of the ion probe-dated structurally lower sequences, supporting the interpretation that both units are separated by a thrust (Papanikolaou, 1978*b*; Bröcker & Pidgeon, 2007). Other studies suggested the existence of a low-angle normal fault (Dürr, 1986; Avigad & Garfunkel, 1991; Avigad *et al.* 1997; Bröcker & Franz, 2006), reactivation of an earlier thrust fault as a normal fault (Bröcker & Pidgeon, 2007) or questioned that a tectonic contact exists at all (P. Gautier, unpub. Ph.D. thesis, Univ. Rennes, 1994 cited in Mehl *et al.* 2007).

On the NE coast, Mehl *et al.* (2007) identified a flat-lying detachment that separates two structural units (Fig. 3a). The rock sequences of the hanging-wall are poorly preserved, but comprise greenschists and serpentinites that are underlain by a basal breccia mainly consisting of serpentinite clasts and minor pelitic schists of the Lower Unit. According to Mehl *et al.* (2007), this Upper Unit is not equivalent to the topmost succession exposed in NW Andros, but represents a distinct tectonic segment of the Upper Cycladic Unit.

3. Sampling strategy

Building on a thin-section collection from a previous study (Bröcker & Franz, 2006), we have focused fieldwork and sampling for further petrographic and mineralogical characterization of the Makrotantalon Unit on the western part of the island. About 200 new thin-sections were prepared for the present study. Two areas located close to the lighthouse near Fasa and on the Aghios Sostis peninsula west of Mermingies (Fig. 2) turned out to be of special significance. Sample locations and petrographic information of key samples from these occurrences are summarized in Figure 2, Tables 1 and 2 and in Table S1 in the online Supplementary Material at http://journals.cambridge.org/geo.

The closure temperature for Sr in white mica is commonly estimated at ~ 500 ± 50 °C (e.g. Cliff, 1985), but this value should only be used with caution, because other factors, such as fluid infiltration, also affect the isotope systematics (e.g. Villa, 1998). In the present case, available information suggests peak metamorphic temperatures of < 500 °C, indicating favourable conditions for dating of tectonometamorphic processes that are largely unaffected by cooling.

Rb–Sr geochronology focused on (a) the presumed contact zone between the Makrotantalon Unit and the Lower Unit and (b) the detachment and uppermost part of the Lower Unit exposed on the NE coast. For this purpose, 11 samples were selected which represent clastic metasediments, calcschists and metabasic schists that were collected within a distance of < 100 m of the presumed shear zones. All samples comprise greenschist-facies mineral assemblages. Sample locations and petrographic information are shown in Figure 2 and in Tables S1 to S3 in the online Supplementary Material at http://journals.cambridge.org/geo. Owing to the lack of a well-constrained tectonic contact between the Makrotantalon Unit and the Lower Unit and the absence of clear lithological and mineralogical differences between both subunits, an unequivocal assignment of samples from the suspected ductile shear zone to the hanging and footwall is extremely difficult or impossible. In NW Andros samples were collected close to occurrences of serpentinites, assuming that the ultramafic rocks mark the tectonic contact. Using the geological map of Papanikolaou (1978*a*) as reference, samples A29 and A33 are part of the Makrotantalon Unit. In order to substantiate the reliability of Cretaceous ages reported in an earlier study of the

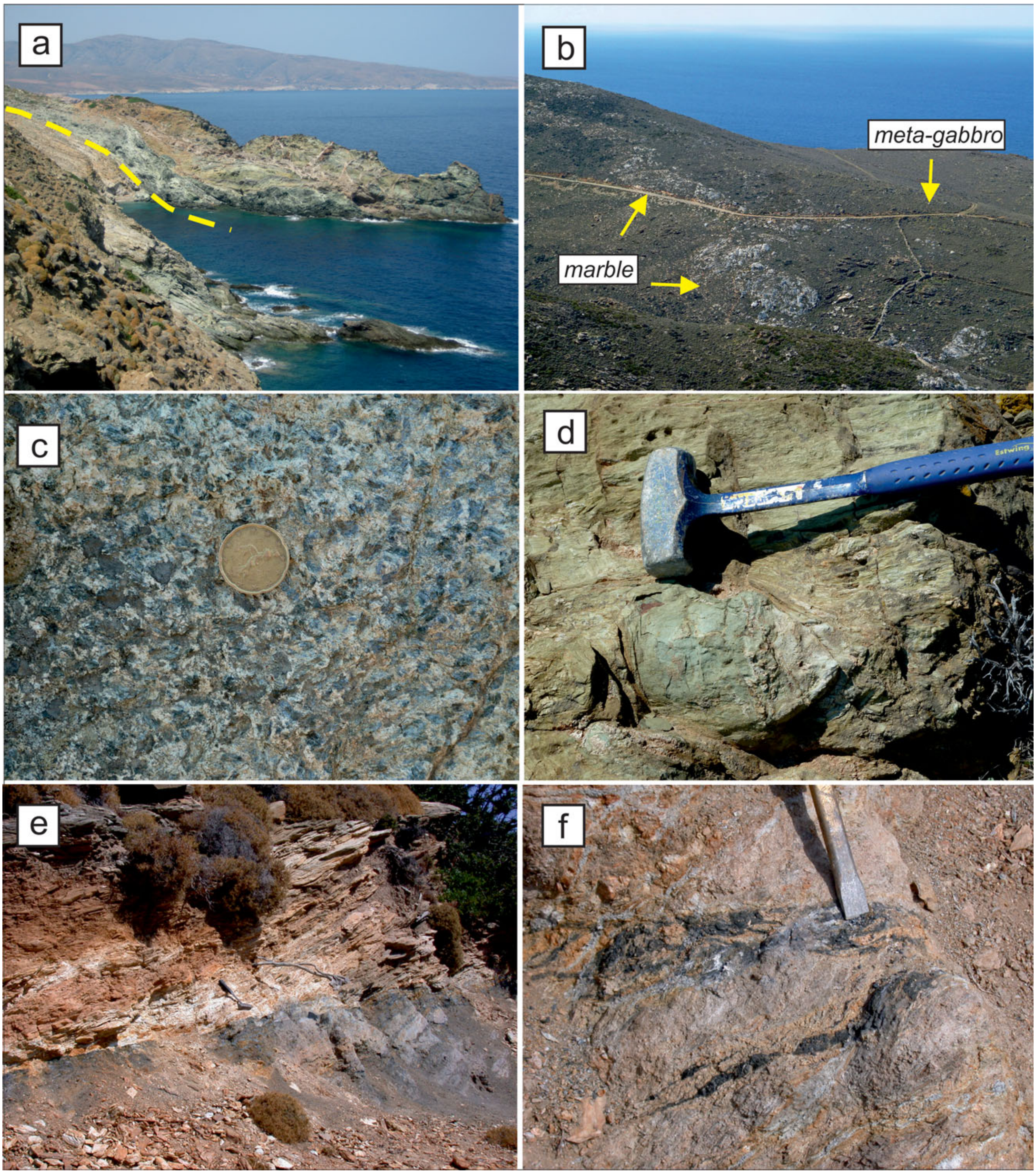

Figure 3. (Colour online) Field photographs from Andros showing (a) the detachment at the NE coast where metasediments of the Lower Unit are tectonically overlain by serpentinites and greenschists of the Upper Unit; (b) view from the lighthouse near Fasa towards the NW, indicating the location of a meta-gabbro block with relict glaucophane; the schists above the marble also locally contain HP relics; (c) close-up of meta-gabbro near Aspro Vouno; (d) metabasic clasts in greenschist matrix on the Aghios Sostis peninsula; (e) and (f) show weak angular unconformity with centimetre-thick veins of cohesive cataclasites cutting through clastic metasediments close to the tectonic contact separating the Makrotantalon Unit from the Lower Unit (star symbol in Fig. 2). Hammer is *c*. 40 cm long, chisel is *c*. 15 cm long and coin is *c*. 2.5 cm diameter.

Makrotantalon Unit (Bröcker & Franz, 2006), additional mineral and/or different grain-size fractions of such samples (samples 1430 and 1839) have also been analysed. All other dated samples are from the Lower Unit, except sample T54 that represents a detachment in NW Tinos. Altogether 14 samples have been newly dated.

4. Analytical methods

Mineral compositions were determined with a JEOL JXA8600MX electron microprobe (EMP) at the Institut für Mineralogie, Universität Münster. Operating conditions were a 15 kV acceleration voltage, 10–15 nA beam current, a spot size of 1–5 μm and a

https://doi.org/10.1017/S0016756813000307 Published online by Cambridge University Press

Table 1. Mineral assemblages of key petrographic samples from the Makrotantalon Unit

Sample	Rock type	gln	Ca-amp	grt	wm	ep/cz	cal	alb	chl	qtz	pmp	laws	tit	rt	cpx	bt/oxy
5737	MS	–	–	–	x	x	–	x	x	x	x	x	x	–	–	x
5645	MS	–	–	–	x	–	–	x	–	x	–	x	–	–	–	x
5658	MA	–	–	–	x	x	–	x	x	x	–	x	x	–	–	x
5719	GS	x	x	–	–	x	–	x	x	x	–	–	x	x	–	x
5720	MS	x	–	–	x	x	–	x	x	x	–	–	x	–	–	x
5734	MS	x	x	–	x	x	–	x	x	x	–	–	x	–	–	x
5748	GS	–	x	–	–	x	–	x	x	x	x	–	x	–	x	x
5751	GS	–	–	–	–	x	–	x	x	x	x	–	–	–	–	x
5781	BS	x	–	–	x	x	–	x	x	x	–	–	x	–	–	–
5784	Q	x	–	x	x	x	–	x	x	x	–	–	x	–	–	x

(± opaques, ± apatite, ± zircon)

Rock abbreviations: MA – meta-acidite; MS – mica schist; GS – greenschist; BS – blueschist; Q – quartzite.
Mineral abbreviations: gln – sodic amphibole; Ca-amp – calcic amphibole; grt – garnet; wm – white mica; ep/cz – epidote/clinozoisite; cal – calcium carbonate; alb – albite; chl – chlorite; qtz – quartz; pmp – pumpellyite; laws – lawsonite; tit – titanite; rt – rutile; cpx – clinopyroxene; bt/oxy – biotite/oxychlorite.

Table 2. Mineral assemblages of samples from Andros that were selected for Rb–Sr dating

Sample	Rock type	gln	Ca-amp	grt	wm	ep/cz	cal	alb	chl	qtz	pmp	laws	tit	rt	cpx	bt/oxy
A7	MA	–	–	–	x	x	–	x	x	x	–	–	x	x	–	–
A10	GS	–	–	x	x	x	–	x	x	x	–	–	x	–	–	x
A12	MA	–	–	–	x	x	x	x	x	x	–	–	–	–	–	–
A17	MS	–	–	–	x	x	x	x	x	x	–	–	x	–	–	x
A18	MS	–	–	–	x	x	x	x	x	x	–	–	x	–	–	x
A22	CS	–	–	–	x	x	x	x	x	x	–	–	–	–	–	–
A27	MS	–	–	–	x	x	x	x	x	x	–	–	–	–	–	x
A29	MA	–	–	–	x	x	x	x	x	x	–	–	x	–	–	x
A33	MS	–	–	–	x	x	x	x	x	x	–	–	–	–	–	x
T54	CS	–	–	–	x	x	x	x	x	x	–	–	–	x	–	–
5636	IM	–	–	–	x	–	x	x	–	x	–	–	–	–	–	–
5657	MS	–	–	x	x	–	–	x	x	x	–	–	x	–	–	x

(± opaques, ± apatite, ± zircon, ± graphite, ± tourmaline)

Rock abbreviations: MA – meta-acidite; MS – mica schist, IM – impure marble; GS – greenschist; CS – calc schist.
Mineral abbreviations: gln – sodic amphibole; Ca-amp – calcic amphibole; grt – garnet; wm – white mica; ep/cz – epidote/clinozoisite; cal – calcium carbonate; alb – albite; chl – chlorite; qtz – quartz; pmp – pumpellyite; laws – lawsonite; tit – titanite; rt – rutile; cpx – clinopyroxene; bt/oxy – biotite/oxychlorite.

counting time of 10 s at the peak and 5 s at the background. Natural mineral standards were used for calibration. The raw data were corrected with a ZAF procedure. Analytical data for blue amphibole, lawsonite, pumpellyite and clinopyroxene is summarized in Tables S2 and S3 in the online Supplementary Material at http://journals.cambridge.org/geo.

To characterize the white mica populations in the studied samples, polished thin-sections were prepared from splits of the phengite separates that were used for white mica dating, with the basal plane of mica plates positioned parallel to the surface of the glass slide. This orientation allowed systematic and representative EMP analysis of core and near rim compositions. For each sample ∼ 20–30 phengite core–rim pairs from the grain-size fractions 355–250 μm and 250–180 μm were analysed (Tables S4 and S5 in online Supplementary Material at http://journals.cambridge.org/geo).

Sample preparation and Rb–Sr thermal ionization mass spectrometric analysis were carried out at the Institut für Mineralogie, Universität Münster. Fresh sample material (1–2 kg) was crushed in a jaw-crusher or steel mortar and an aliquot was ground in a tungsten carbide mill to produce whole-rock powder. The remaining material was further reduced in size using a disc mill. Following sieving into different grain-size fractions, minerals were enriched with a Frantz magnetic separator and/or by adherence to a sheet of paper. In some cases, epidote and titanite were concentrated using bromoform. After fines were removed through additional sieving with a 100 μm mesh, hand-picked mineral concentrates were cleaned in an ultrasonic bath, and repeatedly rinsed in deionized H_2O and ultrapure ethanol. Owing to delicate intergrowth relationships (e.g. epidote and sphene with quartz, albite, phengite) some mineral separates were not completely pure, and quality could not be increased in replicates. If the intergrown phases are in isotopic equilibrium, this does not affect the age, but may result in a slightly higher uncertainty. In the case of disequilibrium, this negatively affects both accuracy and precision.

Whole-rock powders and mineral separates were mixed with a ^{87}Rb–^{84}Sr spike in Teflon screw-top vials and dissolved in a HF–HNO_3 (5:1) mixture on a hotplate overnight. After complete evaporation, 6N HCl was added to the residue. This mixture was again homogenized on a hotplate overnight. After a second evaporation to dryness, Rb and Sr were separated by standard ion exchange procedures (AG 50W-X8 resin) on quartz glass columns using 2.5N HCl as eluent. For mass spectrometric analysis, Rb was loaded with H_2O on Ta filaments; Sr was loaded with TaF_5 on W filaments. Rb and Sr isotopic ratios were determined in static mode using a VG Sector 54 multicollector mass spectrometer (Rb) and a Finnigan Triton multicollector mass spectrometer (Sr). Analyses were carried out in three sessions between 2009 and 2012. The external reproducibility of NBS standard 987 was 0.710218 ± 0.000024 (2σ, n = 32), 0.710200 ± 0.000024 (2σ, n = 26) and 0.710246 ± 0.000032 (2σ, n = 17), respectively. Correction for mass fractionation is based on a $^{86}Sr/^{88}Sr$ ratio of 0.1194. Rb ratios were corrected for mass fractionation using a factor deduced from multiple measurements of NBS standard 607. All ages and elemental concentrations were calculated using the IUGS recommended decay constants (Steiger & Jäger, 1977) by means of Isoplot/Ex 3.22 (Ludwig, 2005). For isochron calculations, $^{87}Rb/^{86}Sr$ and $^{87}Sr/^{86}Sr$ ratios were assigned uncertainties of 1 % (2σ) and 0.005 % (2σ), respectively. Uncertainties of Rb–Sr ages are reported at the 95 % confidence level. Analytical data for different grain-size fractions of phengite, plagioclase, epidote, calcite and whole rocks are summarized in Tables 3 and 4 and depicted in Figures 6, 7 and 8.

5. Results

5.a. Field and petrographic observations

Our studies in NW Andros revealed the following aspects of the local geology (Figs 3, 4):

(a) The Makrotantalon Unit is characterized by rare but unambiguous evidence for blueschist-facies metamorphism at outcrop, hand specimen and thin-section scale. Some samples, especially from the Fasa area, contain relics of Na-amphibole (Fig. 4a, b), mostly with glaucophane-ferroglaucophane composition (Fig. 5a; Table S2 in online Supplementary Material at http://journals.cambridge.org/geo), in association with epidote/clinozoisite and ± garnet. Judging from the field relationships it can be ruled out that these occurrences represent erosional windows exposing rocks of the underlying tectonic unit.

(b) In the same structural position, we have also identified at least one location where a meta-gabbro block (a few metres in size) with well-preserved igneous textures is enclosed in a greenschist-metasediment succession (Fig. 3b). Both the block and the matrix contain relics of sodic amphibole. Similar rock fragments have been found as float. Although only one block has yet been recognized, the field setting and petrographic characteristics are very similar to mélange occurrences with low block abundance, as for example reported from NW Tinos (Bulle *et al*. 2010). Mélanges with metre-sized ophiolitic blocks embedded in schists are also a characteristic feature of the Cycladic Blueschist Unit on Evia (Katzir *et al*. 2000).

(c) Lawsonite has previously not been described from the Makrotantalon Unit, but sporadically occurs in clastic metasediments together with quartz, albite, phengite, chlorite and ± pumpellyite (Fig. 4c–e; Table 1; Table S3 in online Supplementary Material at http://journals.cambridge.org/geo). Lawsonite-bearing samples do not contain relics of sodic amphibole or garnet.

(d) Because of a high degree of overprinting, lack of textural equilibrium and/or absence of white mica, the glaucophane and/or lawsonite-bearing samples found so far are not suitable for Rb–Sr or Ar–Ar multigrain dating.

(e) Near Aghios Sostis (close to the aqua farm buildings), some metabasic rocks of the Makrotantalon Unit still contain relict magmatic clinopyroxene (Fig. 4f) with diopside-augite composition (Fig. 5b; Table S3 in online Supplementary Material at http://journals.cambridge.org/geo). In the same area, some outcrops show pumpellyite-rich metabasic clasts (up to 10 cm) dispersed in a matrix consisting of greenschists (Fig. 3d).

(f) The position of the presumed tectonic contact between the Makrotantalon Unit and Lower Unit is vague and only mapped with low precision, owing to the lack of a well-defined shear zone and the absence of distinct lithological differences or dislocated marker horizons. A key location near Aghios Thomas displays a sharp angular unconformity decorated with centimetre-thick veins of cohesive cataclasites cutting through clastic metasediments (Fig. 3e, f). This outcrop is located in the upper part of the Lower Unit close to serpentinite bodies (Fig. 2) and provides clear evidence for tectonic displacement within the inferred contact zone.

(g) Relics of blue amphibole locally occur in schists considered to belong to the Lower Unit close to the inferred tectonic contact.

5.b. Phengite compositions

Si values in phengitic white mica are pressure dependent (Massonne & Schreyer, 1987) and can be used as a proxy to monitor sample homogeneity. Although compositional variability may not necessarily indicate age heterogeneity, such data provides constraints for interpretation of apparent ages determined on multigrain mineral separates. Heterogeneous mica populations may be compromised by mixing of different growth generations and/or incomplete recrystallization. Dating of such material cannot provide accurate ages, but will only provide an upper age limit for the last overprint.

All white mica populations are characterized by variable inter- and intragrain compositional variations (Figs S1 and S2 in online Supplementary Material, at http://journals.cambridge.org/geo). Si values of phengitic mica range between 3.30 and 3.65 per formula unit (p.f.u.). In most cases, data points of both cores and rims are non-systematically distributed along the ideal mixing line between muscovite and celadonite. Only samples A22 and A27 show a clear separation

https://doi.org/10.1017/S0016756813000307 Published online by Cambridge University Press

Table 3. Rb–Sr isotope results of samples collected in the inferred tectonic contact zone between the Makrotantalon Unit and Lower Unit, NW Andros

Sample	Rock type	Mineral	Grain size (μm)	Rb (ppm)	Sr (ppm)	$^{87}Rb/^{86}Sr$	$^{87}Sr/^{86}Sr$	± 2σ	Age [Ma]
A7	meta-acidite	phengite	355–250	351	271	3.747	0.715910	0.000036	**39.2 ± 1.2 Ma**
A7		phengite	250–180	290	152	5.543	0.716839	0.000036	
A7		phengite	180–125	327	73.5	12.88	0.720920	0.000036	
A7		plagioclase	355–250	15.0	96.1	0.4524	0.713962	0.000036	
A7		plagioclase	250–180	7.6	79.1	0.2796	0.713946	0.000036	
A7		*whole rock*		*65.8*	*298*	*0.6393*	*0.714312*	*0.000036*	
A10	green schist	phengite	250–180	168	63.2	7.693	0.710731	0.000036	**29.8 ± 2.7**
A10		phengite	250–180	208	85.7	7.020	0.710297	0.000036	
A10		phengite	180–125	163	40.7	11.57	0.712313	0.000036	
A10		epidote	180–125	9.8	927	0.03050	0.707428	0.000035	
A27	mica schist	phengite	355–250	376	40.9	26.67	0.741215	0.000037	**43.4 ± 1.1**
A27		phengite	250–180	363	25.9	40.67	0.750034	0.000077	
A27		phengite	250–180	410	26.1	45.59	0.752759	0.000038	
A27		*phengite*	*180–125*	*382*	*29.9*	*37.09*	*0.745191*	*0.000037*	
A27		*plagioclase*	*250–180*	*7.0*	*33.0*	*0.6142*	*0.721510*	*0.000036*	
A29	meta-acidite	phengite	355–250	259	201	3.735	0.716110	0.000036	**41.3 ± 0.8**
A29		phengite	355–250	221	265	2.412	0.715427	0.000036	
A29		phengite	250–180	257	216	3.447	0.716028	0.000036	
A29		phengite	250–180	300	133	6.536	0.717873	0.000036	
A29		phengite	250–180	285	221	3.742	0.716239	0.000036	
A29		phengite	180–125	396	42.7	26.88	0.729774	0.000036	
A29		*epidote*	*180–125*	*22.8*	*975*	*0.06781*	*0.713450*	*0.000036*	
A29		*plagioclase*	*250–180*	*9.2*	*79.7*	*0.3344*	*0.714426*	*0.000036*	
A29		*plagioclase*	*250–180*	*8.8*	*74.4*	*0.3410*	*0.714332*	*0.000036*	
A33	mica schist	phengite	355–250	292	49.9	16.95	0.728976	0.000036	**42.4 ± 3.0**
A33		phengite	355–250	316	36.8	24.86	0.733723	0.000037	
A33		phengite	250–180	336	33.9	28.74	0.736205	0.000037	
A33		phengite	250–180	331	26.5	36.25	0.740412	0.000037	
A33		phengite	180–125	314	44.9	20.24	0.730650	0.000037	
A33		*plagioclase*	*250–180*	*17.4*	*39.7*	*1.271*	*0.721195*	*0.000036*	
A33		*whole rock*		*65.8*	*26.8*	*7.119*	*0.723892*	*0.000036*	
5636	impure marble	phengite	355–250	340	17.1	57.92	0.741628	0.000037	**40.7±0.3 Ma**
5636		phengite	250–180	340	17.0	58.25	0.742113	0.000037	
5636		*phengite*	*180–125*	*345*	*16.3*	*61.33*	*0.742697*	*0.000037*	
5636		calcite	250–180	5.1	1258	0.01175	0.708331	0.000035	
5636		calcite	180–125	5.5	1133	0.01394	0.708335	0.000035	
1430	mica schist	phengite	355–250	387	98.9	11.35	0.732635	0.000037	**104.6 ± 3.8**
1430		phengite	250–180	406	98.8	11.91	0.732949	0.000037	
1430		phengite	250–180	405	101	11.57	0.732656	0.000041	
1430		phengite	250–180	403	99.4	11.77	0.732585	0.000037	
1430		*phengite*	*180–125*	*347*	*63.9*	*15.76*	*0.732948*	*0.000037*	
1430		plagioclase	250–180	7.1	44.2	0.4625	0.716151	0.000036	
1430		plagioclase	250–180	7.0	43.6	0.4679	0.715979	0.000036	
5657	mica schist	phengite	355–250	274	209	3.783	0.723788	0.000036	**87.2 ± 0.8**
5657		phengite	355–250	298	164	5.251	0.725675	0.000036	
5657		phengite	250–180	286	177	4.683	0.725010	0.000036	
5657		*phengite*	*180–125*	*273*	*183*	*4.319*	*0.724707*	*0.000036*	
5657		plagioclase	250–180	9.6	40.0	0.6976	0.720016	0.000036	
5657		plagioclase	180–125	8.9	41.4	0.6246	0.719943	0.000036	
1839	mica schist	phengite	355–250	686	78.4	25.42	0.750316	0.000106	**74.6 ± 2.9**
1839		phengite	355–250	340	132	7.507	0.731433	0.000037	
1839		phengite	250–180	424	57.8	21.28	0.747933	0.000037	**81.5 ± 2.6**
1839		phengite	250–180	432	57.1	21.96	0.748670	0.000037	
1839		*phengite*	*180–125*	*384*	*69.5*	*16.04*	*0.737479*	*0.000037*	
1839		plagioclase	250–180	6.4	19.9	0.9367	0.724514	0.000036	
1839		plagioclase	250–180	7.3	16.8	1.254	0.724573	0.000036	

The $^{87}Rb/^{86}Sr$ ratios were assigned an uncertainty of 1 % (2σ); uncertainties of the $^{87}Sr/^{86}Sr$ ratios are reported at the $2\sigma_m$ level. For the age calculation $^{87}Sr/^{86}Sr$ ratios were assigned an uncertainty of 0.005 % (2σ). Numbers in italics were not used for age calculations. Uncertainties of Rb–Sr ages are reported at the 95 % confidence level.

into two distinct groups of Si values that cluster at ~ 3.55 and ~ 3.43 p.f.u., respectively. In almost all samples, phengite shows a trend of decreasing Si values towards the rim (Figs S1 and S2 in online Supplementary Material at http://journals.cambridge.org/geo), but homogeneous grains representing both compositional groups also occur.

5.c. Rb–Sr-geochronology

Owing to a lack of initial isotopic equilibration and/or subsequent disturbance of the Rb–Sr systematics, most samples show variable degrees of scatter. Linear regression that includes all individual data points yields dates with high uncertainties and mean square weighted

https://doi.org/10.1017/S0016756813000307 Published online by Cambridge University Press

Table 4. Rb–Sr isotope results of samples collected near the detachment exposed on the NE coast of Andros

Sample	Rock type	Mineral	Grain size (μm)	Rb (ppm)	Sr (ppm)	$^{87}Rb/^{86}Sr$	$^{87}Sr/^{86}Sr$	± 2σ	Age [Ma]
A12	meta-acidite	phengite	355–250	266	8.7	88.74	0.745123	0.000037	**26.2 ± 1.0**
A12		phengite	355–250	314	12.3	73.92	0.740084	0.000037	
A12		phengite	180–125	349	11.7	87.06	0.744537	0.000037	
A12		epidote	180–125	34.2	3057	0.03238	0.712202	0.000036	
A12		*whole rock*		*3.8*	*10.0*	*1.089*	*0.711872*	*0.000036*	
A17	mica schist	phengite	355–250	359	8.3	125.6	0.756534	0.000038	**24.4 ± 1.1**
A17		phengite	355–250	368	7.1	150.0	0.765137	0.000038	
A17		phengite	250–180	357	7.9	131.0	0.757666	0.000038	
A17		*phengite*	*180–125*	*357*	*7.1*	*145.6*	*0.760629*	*0.000038*	
A17		titanite	180–125	13.4	146	0.2652	0.712921	0.000036	
A17		*whole rock*		*88.8*	*23.6*	*10.91*	*0.714304*	*0.000036*	
A18	mica schist	phengite	355–250	378	17.0	64.34	0.735379	0.000037	**28.4 ± 0.7**
A18		phengite	250–180	385	13.7	81.45	0.741689	0.000037	
A18		*phengite*	*180–125*	*380*	*13.3*	*82.72*	*0.740588*	*0.000037*	
A18		plagioclase	355–250	8.0	51.2	0.4536	0.709413	0.000035	
A18		plagioclase	250–180	10.0	26.8	1.078	0.709431	0.000035	
A18		titanite	180–125	13.6	54.6	0.7205	0.709446	0.000035	
A18		*whole rock*		*92.1*	*101*	*2.627*	*0.709977*	*0.000035*	
A22	calc schist	phengite	355–250	315	8.4	108.3	0.750285	0.000038	**27.2 ± 1.1**
A22		phengite	250–180	280	7.6	107.5	0.750029	0.000038	
A22		phengite	180–125	256	12.8	57.74	0.730263	0.000037	
A22		calcite + plagioclase	250–180	1.9	169	0.03230	0.708506	0.000035	
A22		*whole rock*		*28.0*	*321*	*0.2523*	*0.708566*	*0.000035*	
T54	calc schist	phengite	355–250	336	36.3	26.79	0.720498	0.000036	**29.2 ± 0.2**
T54		phengite	250–180	355	33.3	30.89	0.722198	0.000036	
T54		*phengite*	*180–125*	*348*	*30.6*	*33.04*	*0.722811*	*0.000036*	
T54		calcite + plagioclase	250–180	6.1	606	0.02908	0.709397	0.000035	

The $^{87}Rb/^{86}Sr$ ratios were assigned an uncertainty of 1 % (2σ); uncertainties of the $^{87}Sr/^{86}Sr$ ratios are reported on the $2\sigma_m$ level. For the age calculation $^{87}Sr/^{86}Sr$ ratios were assigned an uncertainty of 0.005 2>% (2σ). Numbers in italics were not used for age calculations. Uncertainties of Rb–Sr ages are reported at the 95 % confidence level.

deviation (MSWD) values. The variability recorded by these errorchrons is a result of disequilibrium between micas and low Rb/Sr phases (epidote and/or albite) or slight grain-size dependent isotopic variations between different phengite fractions. For example, the 180–125 μm mica fraction often deviates from the best straight-line fit, suggesting a somewhat younger apparent age than observed for the larger grain size. Linear regression that excludes data points obviously recording non-cogenetic formation/recrystallization from age calculations allows the distinguishing of three groups of apparent ages that cluster at ~ 40–43 Ma, ~ 25–30 Ma and ~ 88–105 Ma, respectively.

Group 1: Most samples from the presumed contact zone between the Makrotantalon Unit and the Lower Unit are characterized by Eocene ages (Fig. 6; Table 3). Phengite and calcite data of sample 5636 suggest an age of 40.7 ± 0.3 Ma (MSWD = 0.75, Fig. 6a). For samples A7, A27, A29 and A33 regression lines that are based only on different phengite grain-size fractions yield apparent ages of 39.2 ± 1.2 Ma (MSWD = 6.6), 43.4 ± 1.1 Ma (MSWD = 2.7), 41.3 ± 0.8 Ma (MSWD = 5.4) and 42.4 ± 3.0 Ma (MSWD = 7.2), respectively (Fig. 6b–e). The best straight-line fit for sample A10 indicates the youngest apparent age for a sample from NW Andros (29.8 ± 2.7 Ma, MSWD = 10.3, Fig. 6f).

Group 2: Four samples collected at or close to the detachment at the NE coast yielded Oligocene ages. For samples A12 and A22 linear regression indicates apparent ages of 26.2 ± 1.0 Ma (MSWD = 3.4) and 27.2 ± 1.1 Ma (MSWD = 7.6), respectively (Fig. 7a, d). Alignment of data points of samples A17 and A18 conforms to similar ages of 24.4 ± 1.1 Ma (MSWD = 4) and 28.4 ± 0.7 Ma (MSWD = 33) (Fig. 7b, c). The best straight-line fit for sample T54 from the Tinos detachment yielded an apparent age of 29.2 ± 0.2 Ma (MSWD = 0.00037; Fig. 7e).

Group 3: The internal isochron of sample 5657 from NW Andros indicates an apparent age of 87.2 ± 0.8 Ma (MSWD = 2.2; Fig. 8a). For sample 1430, linear regression suggests an age of 104.6 ± 3.8 Ma (MSWD = 20; Fig. 8b). Because of little variation in the isotopic ratios of different mica grain-size fractions, sample 1430 is effectively a two-point isochron. In the case of sample 1839, combination of plagioclase data points with different mica grain-size fractions leads to regression lines with high MSWD values, suggesting Cretaceous ages (~ 75 Ma and ~ 82 Ma; Fig. 8c).

6. Discussion

6.a. Structural position of the Makrotantalon Unit

Previous studies showed that most parts of Andros can clearly be assigned to the Cycladic Blueschist Unit, but the structural position and metamorphic history of the topmost metamorphic succession (= Makrotantalon Unit) remained uncertain. Papanikolaou (1978*b*,

https://doi.org/10.1017/S0016756813000307 Published online by Cambridge University Press

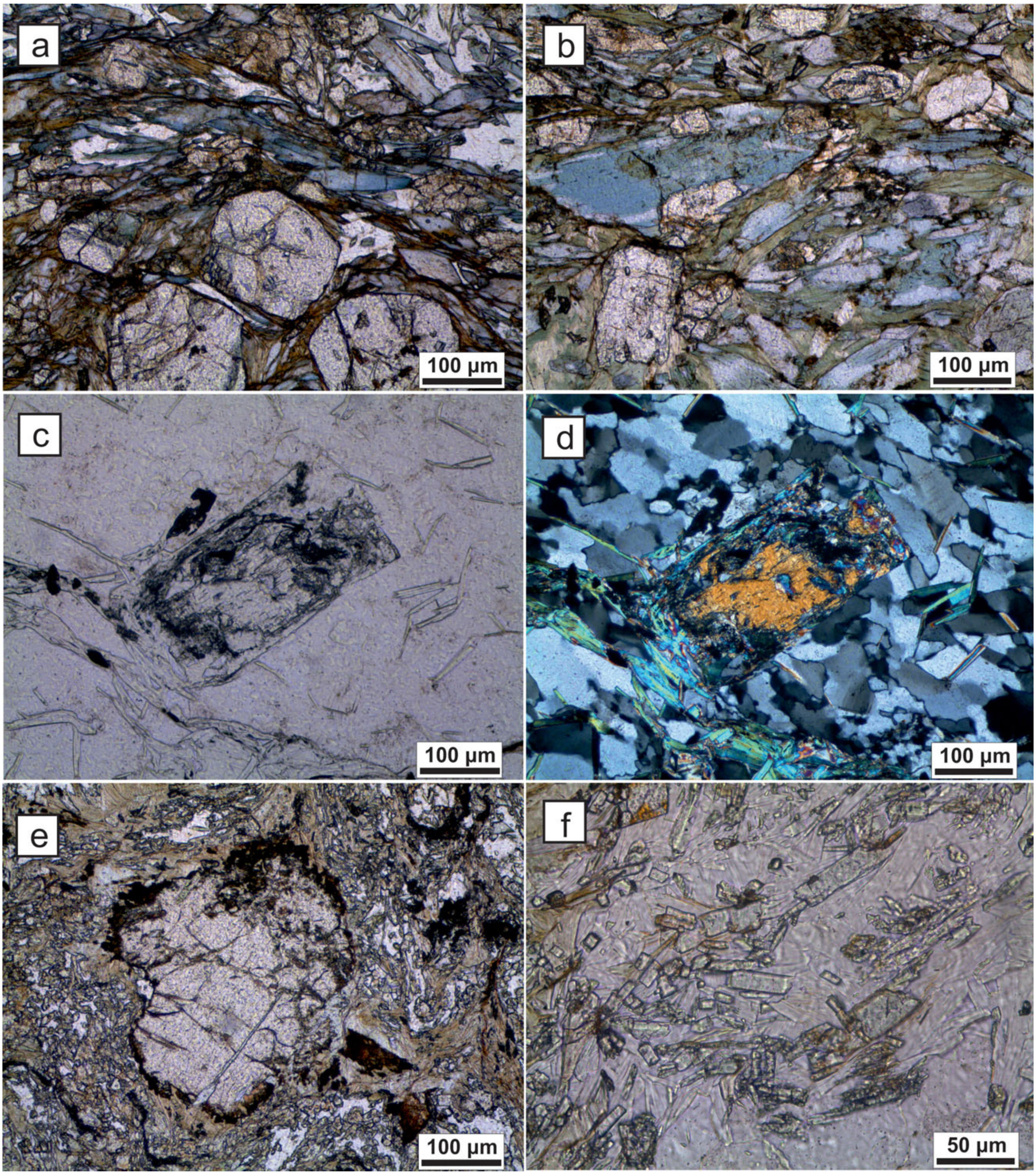

Figure 4. (Colour online) Photomicrographs of samples from the Makrotantalon Unit showing key petrographic features; (a) glaucophane-garnet-epidote (sample 5784); (b) glaucophane-epidote and retrograde chlorite (sample 5719); (c, d) lawsonite (sample 5658; plane-polarized and cross-polarized light), (e) igneous clinopyroxene in greenschist (sample 5748); (f) pumpellyite in lawsonite-bearing quartz mica schist (sample 5737).

1987) suggested a relationship with the Ochi Unit on the neighbouring island of Evia, which belongs to the Cycladic Blueschist Unit. However, owing to the apparent absence of HP/LT relics and the preservation of pre-Tertiary Rb–Sr dates, the Makrotantalon Unit has mostly been interpreted as part of the Upper Cycladic Unit (e.g. Dürr, 1986; Bröcker & Franz, 2006). An alternative explanation has been suggested by Mehl *et al*. (2007), who considered the Makrotantalon Unit either as a subunit of the Cycladic Blueschist Unit that has escaped blueschist-facies re-equilibration, or as an intermediate unit of unknown tectonometamorphic affinity that is squeezed in between the Upper Cycladic Unit and the Cycladic Blueschist Unit.

The present study provides new arguments for this discussion. A significant result of our fieldwork is

https://doi.org/10.1017/S0016756813000307 Published online by Cambridge University Press

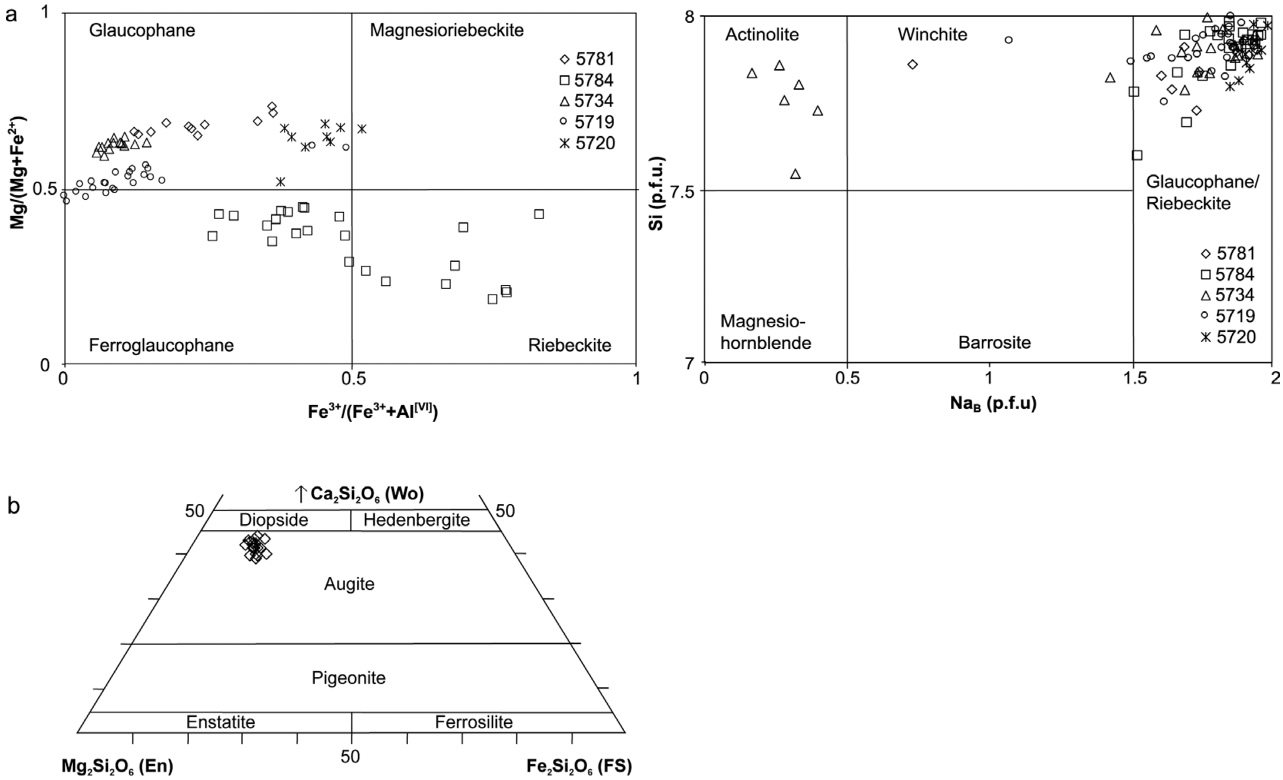

Figure 5. (a) Amphibole classification diagrams (Miyashiro, 1957; Leake *et al*. 1997); (b) Mg–Ca–Fe triangle for pyroxene classification (Morimoto, 1988).

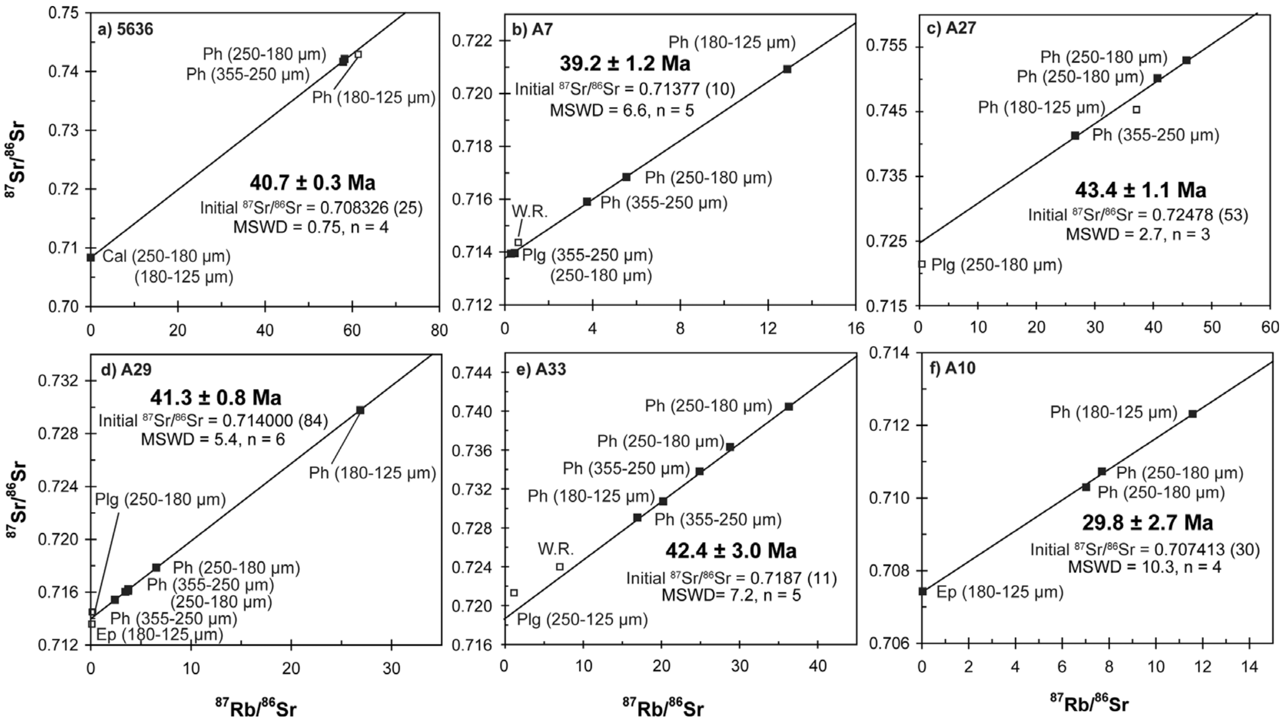

Figure 6. Rb–Sr isochron diagrams for samples from NW Andros (Makrotantalon Unit – Lower Unit contact area). Ph – phengite; Cal – calcite; Ep – epidote/clinozoisite; Plg – plagioclase; W.R. – whole rock. Number in parentheses indicates uncertainty on the last two digits. Analyses indicated by open boxes were not used for isochron calculations.

https://doi.org/10.1017/S0016756813000307 Published online by Cambridge University Press

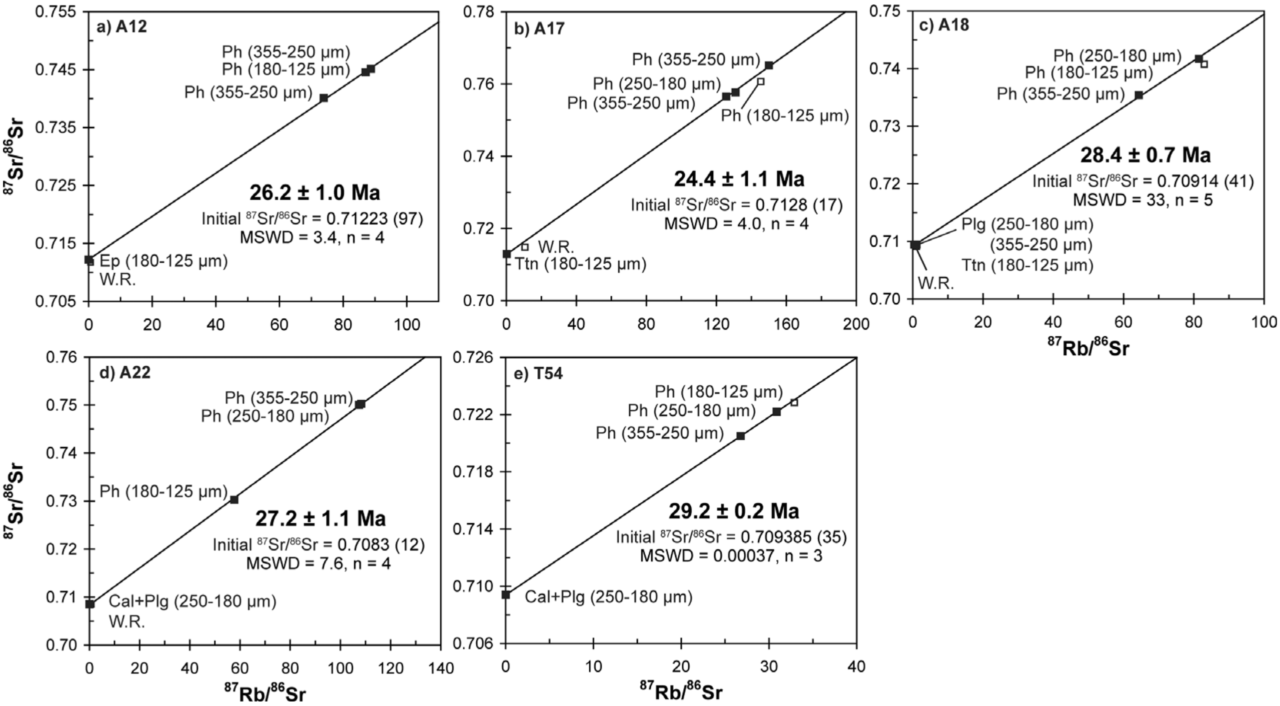

Figure 7. Rb–Sr isochron diagrams for samples from the NE coast of Andros (detachment area). Ph – phengite; Cal – calcite; Ep – epidote/clinozoisite; Plg – plagioclase; W.R. – whole rock. Number in parentheses indicates uncertainty on the last two digits. Analyses indicated by open boxes were not used for isochron calculations.

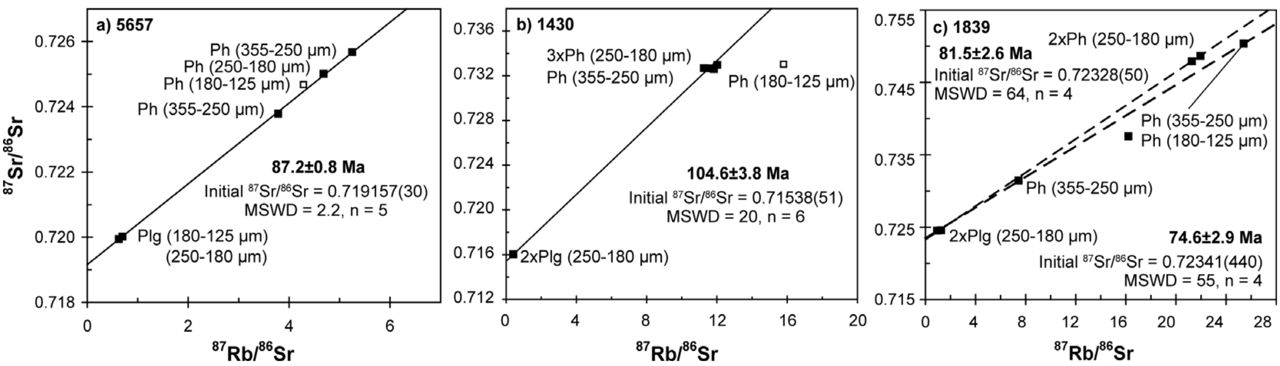

Figure 8. Rb–Sr isochron diagrams for samples from Makrotantalon area indicating pre-Tertiary metamorphic ages. Ph – phengite; Plg – plagioclase. Number in parentheses indicates uncertainty on the last two digits. Analyses indicated by open boxes were not used for isochron calculations.

the discovery of lawsonite- and pumpellyite-bearing parageneses as well as of glaucophane/ferro-glaucophane-epidote-garnet assemblages in rocks that have previously been ascribed to the Makrotantalon Unit (cf. Mehl *et al.* 2007). In the regional context, well-preserved lawsonite has only been described from Evia, where this phase occurs in different rock types of the Cycladic Blueschist Unit (Katzir *et al.* 2000). In other parts of the Cycladic Blueschist Unit, only relics or pseudomorphs after lawsonite are preserved, e.g. on Syros (Sperry, 2000) and Tinos (Bröcker, 1990). Lawsonite is a characteristic phase of LT blueschist-facies conditions (e.g. Clarke, Powell & Fitzherbert, 2006) and the presence of glaucophane-ferroglaucophane in other rocks of the Makrotantalon Unit further supports the interpretation that HP/LT conditions have been reached. The newly found occurrences of blue amphibole were recognized above Permian marbles and thus can unambiguously be assigned to the Makrotantalon Unit. These observations suggest that the Makrotantalon Unit is not part of the upper group of units, but instead represents a tectonic slice belonging to the lower main unit (= Cycladic Blueschist Unit) that has experienced HP/LT metamorphism and widespread, but incomplete, greenschist-facies overprinting. In this context it is noteworthy that Mehl *et al.* (2007) showed on a geological map (fig. 2 of their paper) the distribution of preserved HP/LT paragenesis in areas that partly overlap with the Makrotantalon Unit as mapped by Papanikolaou (1978*a*). Furthermore, Mehl *et al.* (2007) reported the presence of blueschists on either side of the highly deformed serpentinite lens at

https://doi.org/10.1017/S0016756813000307 Published online by Cambridge University Press

Cap Felos, interpreted by us to mark the tectonic contact between the Makrotantalon Unit and Lower Unit. However, these authors emphasized the difficulties in locating the shear zone between both units because the lithologies below and above the contact are very similar. Mehl *et al.* (2007) did not conclude whether or not the Makrotantalon Unit represents a distinct tectonic subunit with a HP/LT history. The reader is left with the impression that the presence of blueschist-facies relics is a distinct characteristic of the Lower Unit.

6.b. Geochronology

The studied rocks record the imprint of a complex sequence of superimposed tectonometamorphic events that have influenced the Rb–Sr isotope characteristics to various degrees. As a consequence, mineral dating documents complex intra-sample relationships that are difficult to deal with. Samples collected close to the presumed tectonic contacts show no straightforward isochron relationships, owing to incomplete resetting of pre-existing mica populations and/or subsequent disturbance of the isotope systems. The observed age scatter cannot exclusively be linked to localized deformation and associated fluid–rock interaction in a shear zone, but may evidence a significant contribution imposed by regional greenschist-facies overprinting (~ 23–21 Ma; Bröcker & Franz, 2006), or even younger processes. The lack of isotopic equilibrium and the range in Si values of phengites suggests that the apparent ages may be compromised by mixing of different growth generations and/or inheritance from earlier metamorphic events. Multigrain dating of such populations can only yield upper limits for the overprinting process that has caused partial recrystallization. Although of limited use for accurate and precise dating of distinct geological processes, the new dataset still provides helpful insights for interpretation of the geochronological evolution of Andros.

6.b.1. Indications for Cretaceous metamorphism in the Makrotantalon Unit

Not yet fully explained is the importance of Cretaceous Rb–Sr white mica dates (~ 74–104 Ma) of greenschist-facies rocks from the Makrotantalon Unit (Bröcker & Franz, 2006; this study). The presence of such rocks is confirmed by newly dated sample 5657, and seems to be supported by additional data for two previously dated samples, although the potential significance of the latter is compromised by poor precision and high MSWD values. Such ages are completely unknown from the HP/LT rocks and their overprinted derivatives cropping out on the central Aegean islands. The preservation of Cretaceous ages in the Makrotantalon Unit might be related to regional differences in the *P–T–d* history or to a different duration of metamorphic overprinting (cf. Katzir *et al.* 2000), which failed to completely eliminate inherited ages.

Potential candidates for rocks recording age inheritance occur on Evia, where apparently lower-grade HP/LT rocks are exposed in several tectonic subunits (Styra, Ochi and Tsaki nappes) of the South Evia Blueschist Belt. This belt is considered to represent the northern extension of the eclogite-blueschist association exposed on Syros, Sifnos and Tinos (e.g. Shaked, Avigad & Garfunkel, 2000; Katzir *et al.* 2000). The lithology comprises various types of clastic metasediments, impure marbles, felsic and basic meta-igneous rocks as well as block-in-matrix associations with variably sized ultrabasic and metabasic rocks enclosed in metasedimentary and serpentinitic host rocks (Shaked, Avigad & Garfunkel, 2000; Katzir *et al.* 2000). Zircons from meta-acidic rocks representing the structurally coherent sequences yielded ID-TIMS U–Pb single grain ages of ~ 234–232 Ma and ~ 214 Ma, which were interpreted to constrain the formation of the igneous protolith in Late Triassic times (Chatzaras *et al.* 2012).

Several studies suggested lower *P–T* conditions for the HP stage recorded in the South Evia Blueschist Belt (~ 8–11 kbar and 300–420 °C; Bonneau & Kienast, 1982; Reinecke, 1986; Klein-Helmkamp, Reinecke & Stöckert, 1995) than reported from the central Aegean islands (~ 12–20 kbar, ~ 450–550 °C, e.g. Bröcker *et al.* 1993; Trotet, Vidal & Jolivet, 2001; Bulle *et al.* 2010). More recent *P–T* estimates indicate that the HP rocks on Evia have reached the field of the epidote–blueschist facies (10–12 kbar and 380–450 °C, Lensky *et al.* 1997; > 11 kbar and 400–450 °C, Katzir *et al.* 2000), but that temperatures either were slightly lower than in other parts of the Cyclades or that, owing to a shorter residence time at similar metamorphic conditions, a complete equilibration to the prevailing temperature regime did not occur (Katzir *et al.* 2000). HP/LT rocks mostly yielded $^{40}Ar–^{39}Ar$ ages of ~ 55–45 Ma (Maluski *et al.* 1981), but younger ages (~ 35–27 Ma) were reported for mylonitic samples from distinct shear zones (Ring *et al.* 2007). A systematic study of metamorphic ages recorded in the dominant schist-quartzite-meta-granitoid succession that forms large parts of southern Evia has not yet been carried out. Remarkable are yet unconfirmed Rb–Sr dates of ~ 75–93 Ma for structurally controlled microsamples from this rock suite (M. Wegmann, unpub. Ph.D. thesis, Freie Univ. Berlin, 2006). This issue needs a more detailed examination in future studies.

The results of our study suggest that the Makrotantalon Unit is a subunit of the Cycladic Blueschist Unit. Geographical vicinity, field and petrological characteristics are in accordance with models suggesting a correlation with the HP/LT nappe stack exposed in southern Evia (Papanikolaou, 1978*b*). However, although available observations and data indicate an affinity to the South Evia Blueschist Belt, a clear relationship to a specific tectonic slice on Evia is so far uncertain. It is well possible that the Makrotantalon Unit has no direct lateral counterpart on Evia, but represents an independent tectonic subunit within a more complex nappe stack than presently acknowledged.

https://doi.org/10.1017/S0016756813000307 Published online by Cambridge University Press

6.b.2. Rb–Sr dates of other samples collected in NW Andros

In most parts of northern Andros evidence for a narrow high-strain zone separating distinct tectonic subunits has not yet been identified, possibly owing to subsequent metamorphic overprinting, associated recrystallization and formation of new mineral assemblages. The position of the inferred ductile shear zone is best approximated by a discontinuous belt of serpentinites in the upper part of the metamorphic section that can be traced across the island. Petrographic characteristics of samples selected from this structural position suggest complete greenschist-facies overprinting, but intra-sample isotopic equilibrium including all studied phases is obviously not given. Nevertheless, the picture emerging from the new petrographic and isotopic results can be plausibly reconciled with observations made in the regional context.

On several Cycladic islands (e.g. Syros, Tinos, Sifnos) the best preserved HP/LT rocks occur in the upper part of the metamorphic succession, whereas the highest degree of overprinting and the largest domains of greenschist-facies rocks are found at lower lithostratigraphic positions (e.g. Bröcker, 1990; Bröcker & Franz, 1998; Trotet, Vidal & Jolivet, 2001). Such field relations have been related to more pervasive fluid infiltration in the basal parts. On Andros, field, petrographic and geochronological data indicate a similar situation, but with a more cryptic top-to-bottom gradient than observed on other islands. Within a predominantly greenschist-facies setting, only few and widely scattered occurrences with HP/LT relics can be found. One of the best locations for preserved HP rocks is exposed at Cap Felos in the topmost part of the Lower Unit, directly below a prominent serpentinite ridge (Mukhin, 1996). At a similar lithostratigraphic position, relics of Na-amphibole are sporadically preserved in other parts of the island, but petrographic evidence for an earlier HP stage has mostly been erased by greenschist-facies overprinting. In spite of that field situation, the Rb–Sr isotope system of phengitic mica has apparently retained memory of the HP/LT event. For five out of six samples from this lithostratigraphic position, white mica grain-size fractions indicate apparent Rb–Sr ages of ~ 40 Ma, which fall within the lower age range reported for blueschist-facies rocks of the Cyclades (e.g. Bröcker *et al*. 1993). At lower lithostratigraphic levels more pervasive retrogression and recrystallization has mostly eliminated petrographic evidence for this event and the Rb–Sr isotope system is more strongly reset (Bröcker & Franz, 2006).

6.b.3. Timing of tectonic emplacement

Fossils in dolomitic marbles of the Makrotantalon Unit yielded Permian ages (Papanikolaou, 1978*b*). U–Pb dating of detrital zircon indicates maximum depositional ages of ~ 260 Ma for the Makrotantalon Unit and of ~ 170–160 Ma for the Lower Unit (M. H. Huyskens, unpub. data). These age constraints are consistent with previous interpretations suggesting an inverted tectonostratigraphy – rocks at the top of the succession are older than the structurally lower sequences – implying that the contact between both subunits originated as a thrust during synorogenic convergence. The widespread lack of a recognizable shear zone may be owing to a combination of metamorphic overprinting of the original zone of mylonitization and the absence of significant lateral displacement during exhumation. The degree to which this contact has later been reactivated as a low-angle normal shear zone (Bröcker & Pidgeon, 2007) is not clearly determined. Findings of cataclasites in some segments of the tectonic contact are interpreted to indicate such deformation increments. It is here suggested that this zone mainly operated as a thrust and that the ~ 40 Ma ages recorded in samples from this zone provide a lower time limit for final movement and mica recrystallization coupled to this process.

6.b.4. Rb–Sr ages of samples collected on the NE coast of Andros

In some outcrops along the NE coast, a flat-lying detachment is exposed that cuts through the topmost part of the metamorphic succession, separating two distinct structural units (Mehl *et al*. 2007). Owing to restricted outcrop size and limited exposure of the hangingwall sequences, it remains unclear if this shear zone represents a more strongly reactivated equivalent to the tectonic contact in NW Andros, or a completely different shear zone. There seem to be some differences in the lithostratigraphy of the footwall sequence, e.g. a prominent marble horizon is lacking, supporting the interpretation that this is a different tectonic contact.

On the neighbouring island of Tinos, a NE-dipping detachment separates an Upper Unit that is comprised of phyllites, metagabbros, ophicalcites and serpentinites from rock sequences of the Cycladic Blueschist Unit (e.g. Zeffren *et al*. 2005). On Tinos, previous studies documented heterogeneous age resetting towards the base of the hangingwall during Tertiary times (Bröcker & Franz, 1998; Zeffren *et al*. 2005), but no systematic dating study has been carried out on the footwall part close to the shear zone. On Andros, samples collected directly at or in the footwall close to the detachment, yielded a relatively narrow range of apparent ages (~ 29–25 Ma). Although this cannot yet unambiguously be documented, we consider it very likely that the ~ 29–25 Ma age group approximates the time of a prominent ductile increment along this shear zone under greenschist-facies conditions.

The Rb–Sr age from the detachment in northern Tinos (~ 30 Ma) corresponds very well to the results obtained on samples from NE Andros, but on Tinos the situation is more complex. The tectonic contact juxtaposing the Upper Unit onto the Lower Unit is exposed in several widely separated locations across the island, which record different increments of ductile deformation along the shear zone ranging from ~ 30 Ma in the northern part to at least ~ 21 Ma in the southern part of Tinos (Bröcker & Franz, 1998). It is noteworthy that on Evia, where lower parts of the Cycladic nappe stack are exposed, Rb–Sr geochronology of HP mylonites from different shear zones yielded ages of ~ 33–27 Ma, which were interpreted to bracket the time span of mylonitization-related isotopic re-equilibration under late blueschist-facies conditions (Ring *et al*. 2007).

7. Conclusions

The status of the Makrotantalon Unit within the framework of the Cycladic nappe stack has previously not clearly been determined. Mehl *et al*. (2007) summarized the results of earlier research and concluded that only two plausible interpretations are supported by the data available at that time: (1) the Makrotantalon Unit belongs to the Cycladic Blueschist Unit but did not experience blueschist-facies re-equilibration, or (2) the Makrotantalon Unit is a distinct unit juxtaposed between the Upper Cycladic Unit and the Lower Unit. The results of our study ascertain the importance of a third alternative: the Makrotantalon Unit is part of the Cycladic Blueschist Unit and underwent a corresponding metamorphic history. In contrast to the widely held view that the topmost rock sequences on Andros only experienced low- to medium-grade *P–T* conditions (e.g. Bröcker & Franz, 2006), we document unambiguous evidence for earlier HP/LT metamorphism. On a regional scale, correlation with the South Evia Blueschist Belt is very likely, but assignment to a specific subunit is as yet unconfirmed. The Makrotantalon Unit may even represent an independent tectonic subunit without direct counterpart in the nappe stack exposed on Evia. The tectonic contact between the Makrotantalon Unit and the Lower Unit originated as a thrust. Clear evidence for widespread and sustained reactivation as a flat-lying normal shear zone during regional extension has not been found. Direct dating of distinct displacement along this shear zone has not been possible, but a lower age limit of ~ 40 Ma for final thrusting is constrained by the preservation of an inherited Rb–Sr age signature. Sporadically preserved Cretaceous ages are the legacy of earlier metamorphic events. The detachment on the NE coast of Andros records a different aspect of the structural evolution and accommodates extension-related deformation from ductile to brittle conditions. Rb–Sr ages (~ 29–25 Ma) of greenschist-facies samples collected close to or at this fault are considered to closely delimit the time of a distinct increment of ductile deformation along this shear zone.

Acknowledgements. We thank H. Baier for her help with the isotope analyses and J. Berndt for his support on the electron microprobe. Reviews by D. Avigad and an anonymous reviewer are appreciated.

References

Altherr, R., Kreuzer, H., Wendt, I., Lenz, H., Wagner, G. A., Keller, J., Harre, W. & Höhndorf, A. 1982. A Late Oligocene/Early Miocene high temperature belt in the Attic-Cycladic Crystalline Complex (SE Pelagonian, Greece). *Geologisches Jahrbuch* **E 23**, 97–164.

Altherr, R., Schliestedt, M., Okrusch, M., Seidel, E., Kreuzer, H., Harre, W., Lenz, H., Wendt, I. & Wagner, G. A. 1979. Geochronology of high-pressure rocks on Sifnos (Cyclades, Greece). *Contributions to Mineralogy and Petrology* **70**, 245–55.

Avigad, D. & Garfunkel, Z. 1989. Low angle shear zones underneath and above a blueschist belt – Tinos Island, Cyclades, Greece. *Terra Nova* **1**, 182–7.

Avigad, D. & Garfunkel, Z. 1991. Uplift and exhumation of high-pressure metamorphic terrains; the example of the Cycladic blueschist belt (Aegean Sea). *Tectonophysics* **188**, 357–72.

Avigad, D., Garfunkel, Z., Jolivet, L. & Azanon, J. M. 1997. Back arc extension and denudation of Mediterranean eclogites. *Tectonics* **16**, 924–41.

Bonneau, M. & Kienast, J. R. 1982. Subduction, collision et schistes bleus (Grece). *Bulletin de la Société geologique de France* **24**, 781–91.

Bröcker, M. 1990. Blueschist-to-greenschist transition in metabasites from Tinos Island (Cyclades, Greece): compositional control or fluid infiltration. *Lithos* **25**, 25–39.

Bröcker, M., Bieling, D., Hacker, B. & Gans, P. 2004. High-Si phengite records the time of greenschist-facies overprinting: implications for models suggesting mega-detachments in the Aegean Sea. *Journal of Metamorphic Geology* **22**, 427–42.

Bröcker, M. & Enders, M. 1999. U–Pb zircon geochronology of unusual eclogite-facies rocks from Syros and Tinos (Cyclades, Greece). *Geological Magazine* **136**, 111–18.

Bröcker, M. & Franz, L. 1998. Rb–Sr isotope studies on Tinos Island (Cyclades, Greece): additional time constraints for metamorphism, extent of infiltration-controlled overprinting and deformational activity. *Geological Magazine* **135**, 369–82.

Bröcker, M. & Franz, L. 2005. The base of the Cycladic blueschist unit on Tinos Island (Greece) re-visited: field relationships, phengite chemistry and Rb–Sr geochronology. *Neues Jahrbuch für Mineralogie Abhandlungen* **181/1**, 81–93.

Bröcker, M. & Franz, L. 2006. Dating metamorphism and tectonic juxtaposition on Andros Island (Cyclades, Greece): results of a Rb–Sr study. *Geological Magazine* **143**, 609–20.

Bröcker, M. & Keasling, A. 2006. Ionprobe U–Pb zircon ages from the high-pressure/low-temperature mélange of Syros, Greece: age diversity and the importance of pre-Eocene subduction. *Journal of Metamorphic Geology* **24**, 615–31.

Bröcker, M., Kreuzer, H., Matthews, A. & Okrusch, M. 1993. $^{40}Ar/^{39}Ar$ and oxygen isotope studies of polymetamorphism from Tinos Island, Cycladic blueschist belt. *Journal of Metamorphic Geology* **11**, 223–40.

Bröcker, M. & Pidgeon, R. T. 2007. Protolith ages of meta-igneous and meta-tuffaceous rocks from the Cycladic blueschist unit, Greece: results of a reconnaissance U–Pb zircon study. *Journal of Geology* **115**, 83–98.

Buick, I. S. & Holland, T. J. B. 1989. The P–T– t path associated with crustal extension, Naxos, Cyclades, Greece. In *Evolution of Metamorphic Belts* (eds J. S. Daly,

https://doi.org/10.1017/S0016756813000307 Published online by Cambridge University Press

R. A. Cliff & B. W. D. Yardley), pp. 365–9. Geological Society of London, Special Publication no. 43.

BULLE, F., BRÖCKER, M., GÄRTNER, C. & KEASLING, A. 2010. Geochemistry and geochronology of HP mélanges from Tinos and Andros, Cycladic blueschist belt, Greece. *Lithos* **117**, 61–81.

BUZAGLO-YORESH, A., MATTHEWS, A. & GARFUNKEL, Z. 1995. Metamorphic evolution on Andros and Tinos – a comparative study. In *Israel Geological Society Annual Meeting 1995* (eds Y. Arkin & D. Avigad), p. 16. Jerusalem: Israel Geological Society.

CHATZARAS, V., DÖRR, W., FINGER, F., XYPOLIAS, P. & ZULAUF, G. 2012. U–Pb single zircon ages and geochemistry of metagranitoid rocks in the Cycladic Blueschists (Evia Island): implications for the Triassic tectonic setting of Greece. *Tectonophysics* **595–6**, 125–39.

CLARKE, G. L., POWELL, R. & FITZHERBERT, J. A. 2006. The lawsonite paradox: a comparison of field evidence and mineral equilibria modelling. *Journal of Metamorphic Geology* **24**, 715–25.

CLIFF, R. A. 1985. Isotopic dating in metamorphic belts. *Journal of the Geological Society, London* **142**, 97–110.

DÜRR, S. 1986. Das Attisch-kykladische Kristallin. In *Geologie von Griechenland* (ed. V. Jacobshagen), pp. 116–49. Gebrüder Borntraeger.

DÜRR, S., ALTHERR, R., KELLER, J., OKRUSCH, M. & SEIDEL, E. 1978. The Median Aegean Crystalline Belt: stratigraphy, structure, metamorphism, magmatism. In *Alps, Apennines, Hellenides* (eds H. Closs, D. H. Roeder & K. Schmidt), pp. 455–77. IUGS Report no.38. Stuttgart: Schweizerbart.

FU, B., VALLEY, J. W., KITA, N. T., SPICUZZA, M. J., PATON, C., TSUJIMORI, T., BRÖCKER, M. & HARLOW, G. E. 2010. Multiple origins of zircons in jadeitite. *Contributions to Mineralogy and Petrology* **159**, 769–80.

GÄRTNER, C., BRÖCKER, M., STRAUSS, H. & FARBER, K. 2011. Strontium, carbon and oxygen isotope geochemistry of marbles from the Cycladic blueschist belt, Greece. *Geological Magazine* **148**, 511–28.

GAUTIER, P. & BRUN, J. P. 1994*a*. Crustal-scale geometry and kinematics of late-orogenic extension in the central Aegean (Cyclades and Evia Island). *Tectonophysics* **238**, 399–424.

GAUTIER, P. & BRUN, J. P. 1994*b*. Ductile crust exhumation and extensional detachments in the central Aegean (Cyclades and Evia islands). *Geodinamica Acta* **7**, 57–85.

GAUTIER, P., BRUN, J. P., MORICEAU, R., SOKOUTIS, D., MARTINOD, J. & JOLIVET, L. 1999. Timing, kinematics and cause of Aegean extension: a scenario based on a comparison with simple analogue experiments. *Tectonophysics* **315**, 31–72.

KATZIR, Y., AVIGAD, D., MATTHEWS, A., GARFUNKEL, Z. & EVANS, B. W. 2000. Origin, HP/LT metamorphism and cooling of ophiolitic melanges in southern Evia (NW Cyclades), Greece. *Journal of Metamorphic Geology* **18**, 699–718.

KEAY, S. & LISTER, G. 2002. African provenance for the metasediments and metaigneous rocks of the Cyclades, Aegean Sea, Greece. *Geology* **30**, 235–38.

KLEIN-HELMKAMP, U., REINECKE, T. & STÖCKERT, B. 1995. The aragonite–calcite-transition in LT–HP metamorphic carbonatic rocks from S-Evia, Greece: the microstructural and compositional record. *Bochumer Geologische und Geotechnische Arbeiten* **44**, 78–83.

LEAKE, B. E., WOOLLEY, A. R., ARPS, C. E. S., BIRCH, W. D., GILBERT, M. C., GRICE, J. D., HAWTHORNE, F. C., KATO, A., MANDARINO, J. A., MARESCH, W. V., NIKEL, E. H., ROCK, N. M. S., SCHUMACHER, J. C., SMITH, D. C., STEPHENSON, N. C. N., UNGARETTI, L., WHITTAKER, E. J. W. & YOUZHI, G. 1997. Nomenclature of amphiboles: report of the Subcommittee on Amphiboles of the International Mineralogical Association, Commission on New Minerals and Mineral Names. *American Mineralogist* **82**, 1019–37.

LENSKY, N., AVIGAD, D., GARFUNKEL, Z. & EVANS, B. W. 1997. The tectono-metamorphic evolution of blueschists in South Evia, Hellenide Orogenic belt (Greece). *Israel Geological Society, Annual Meeting 1997*, 66–67.

LUDWIG, K. R. 2005. *User's Manual for ISOPLOT/Ex 3.22. A Geochronological Toolkit for Microsoft Excel*. Berkeley Geochronology Center Special Publication, pp. 71.

MALUSKI, H., VERGELY, P., BAVAY, D., BAVAY, P. & KATSIKATSOS, G. 1981. $^{39}Ar/^{40}Ar$ dating of glaucophanes and phengites in southern Euboa (Greece) geodynamic implications. *Bulletin de la Société géologique de France* **5**, 469–76.

MASSONNE, H. J. & SCHREYER, W. 1987 Phengite geobarometry based on the limiting assemblage with K-feldspar, phlogopite, and quartz. *Contributions to Mineralogy and Petrology* **96**, 212–24.

MATTHEWS, A. & SCHLIESTEDT, M. 1984. Evolution of the blueschist and greenschist facies rocks of Sifnos, Cyclades, Greece. A stable isotope study of subduction related metamorphism. *Contributions to Mineralogy and Petrology* **88**, 150–63.

MEHL, C., JOLIVET, L., LACOMBE, O., LABROUSSE, L. & RIMMELE, G. 2007. Structural evolution of Andros (Cyclades, Greece): a key to the behaviour of a (flat) detachment within an extending continental crust. In *The Geodynamics of the Aegean and Anatolia* (eds T. Taymaz, Y. Yilmaz & Y. Dilek), pp. 41–73. Geological Society of London, Special Publication no. 291.

MIYASHIRO, A. 1957. The chemistry, optics and genesis of the alkali-amphiboles. *Journal of Faculty of Science, University of Tokyo* **11**, 57–83.

MORIMOTO, N. 1988. Nomenclature of pyroxenes. *Mineralogical Magazine* **52**, 535–50.

MUKHIN, P. 1996. The metamorphosed olistostromes and turbidites of Andros Island, Greece, and their tectonic significance. *Geological Magazine* **133**, 697–711.

OKRUSCH, M. & BRÖCKER, M. 1990. Eclogite facies rocks in the Cycladic blueschist belt, Greece: a review. *European Journal of Mineralogy* **2**, 451–78.

PAPANIKOLAOU, D. 1978*a*. *Geologic Map of Greece. Andros Sheet*. I.G.M.E. (Institute of Geology and Mineral Exploration, gen. di. V. Andronopoulos).

PAPANIKOLAOU, D. 1978*b*. Contribution to the geology of the Aegean Sea; the island of Andros. *Annales Geologiques des Pays Helleniques* **29** (2), 477–553.

PAPANIKOLAOU, D. 1987. Tectonic evolution of the Cycladic blueschist belt (Aegean Sea, Greece). In *Chemical Transport in Metasomatic Processes* (ed. H. C. Helgeson), pp. 429–50. NATO ASI series. Dordrecht: Reidel.

PARRA, T., VIDAL, O. & JOLIVET, L. 2002. Relation between the intensity of deformation and retrogression in blueschist metapelites of Tinos Island (Greece) evidenced by chlorite-mica local equilibria. *Lithos* **63**, 41–66.

PATZAK, M., OKRUSCH, M. & KREUZER, H. 1994. The Akrotiri unit on the island of Tinos, Cyclades, Greece: witness to a lost terrane of Late Cretaceous age. *Neues Jahrbuch für Geologie und Paläontologie Abhandlungen* **194**, 211–52.

Putlitz, B., Cosca, M. A. & Schumacher, J. C. 2005. Prograde mica $^{40}Ar/^{39}Ar$ growth ages recorded in high pressure rocks (Syros, Cyclades, Greece). *Chemical Geology* **214**, 79–98.

Reinecke, T. 1982. Cymrite and celsian in manganese-rich metamorphic rocks from Andros island, Greece. *Contributions to Mineralogy and Petrology* **79**, 333–6.

Reinecke, T. 1986. Phase relationships of sursassite and other Mn-silicates in highly oxidized, high-pressure metamorphic rocks from Evia and Andros Islands, Greece. *Contributions to Mineralogy and Petrology* **94**, 110–26.

Reinecke, T., Okrusch, M. & Richter, P. 1985. Geochemistry of ferromanganoan metasediments from the island of Andros, Cycladic Blueschist Belt, Greece. *Chemical Geology* **53**, 249–78.

Ring, U., Glodny, J., Will, T. & Thomson, S. 2007. An Oligocene extrusion wedge of blueschist-facies nappes on Evia Island, Aegean Sea, Greece: implications for the early exhumation of high-pressure rocks. *Journal of Geological Society, London* **164**, 637–57.

Ring, U., Glodny, J., Will, T. & Thomson, S. 2010. The Hellenic subduction system: high-pressure metamorphism, exhumation, normal shear zoning, and large-scale extension. *Annual Review of Earth and Planetary Sciences* **38**, 45–76.

Shaked, Y., Avigad, D. & Garfunkel, Z. 2000. Alpine high-pressure metamorphism at the Almyropotamos window (southern Evia, Greece). *Geological Magazine* **137**, 367–80.

Sperry, A. 2000. Pseudomorphs after lawsonite as an indication of pressure-temperature evolution in blueschists from Syros, Greece. *13th Keck Symposium Volume*, pp. 52–5. Keck Geology Consortium.

Steiger, R. H. & Jäger, E. 1977. Subcommission on geochronology: convention on the use of decay constants in geo- and cosmochronology. *Earth and Planetary Science Letters* **36**, 359–62.

Trotet, F., Vidal, O. & Jolivet, L. 2001. Exhumation of Syros and Sifnos metamorphic rocks (Cyclades, Greece). New constraints on the P–T paths. *European Journal of Mineralogy* **13**, 901–20.

Villa, I. M. 1998. Isotopic closure. *Terra Nova* **10**, 42–7.

Wijbrans, J. R. & McDougall, I. 1988. Metamorphic evolution of the Attic Cycladic Metamorphic Belt on Naxos (Cyclades, Greece) utilizing $^{40}Ar/^{39}Ar$ age spectrum measurements. *Journal of Metamorphic Geology* **6**, 571–94.

Wijbrans, J. R., Schliestedt, M. & York, D. 1990. Single grain argon laser probe dating of phengites from the blueschist to greenschist transition on Sifnos (Cyclades, Greece). *Contributions to Mineralogy and Petrology* **104**, 582–93.

Zeffren, S., Avigad, D., Heimann, A. & Gvirtzman, Z. 2005. Age resetting of hanging wall rocks above a low-angle detachment shear zone: Tinos Island (Aegean Sea). *Tectonophysics* **400**, 1–25.

Ziv, A., Katzir, Y., Avigad, D. & Garfunkel, Z. 2010. Strain development and kinematic significance of the Alpine folding on Andros (western Cyclades, Greece). *Tectonophysics* **488**, 248–55.